

Effective Semi-Supervised Node Classification on Few-Labeled Graph Data

Ziang Zhou
fduscottzhou@outlook.com
The Hong Kong Polytechnic
University
China

Jieming Shi
jieming.shi@polyu.edu.hk
The Hong Kong Polytechnic
University
China

Shengzhong Zhang
szzhang17@fudan.edu.cn
Fudan University
China

Zengfeng Huang
huangzf@fudan.edu.cn
Fudan University
China

Qing Li
csqli@comp.polyu.edu.hk
The Hong Kong Polytechnic
University
China

ABSTRACT

Graph neural networks (GNNs) are designed for *semi-supervised node classification* on graphs where only a small subset of nodes have class labels. However, under extreme cases when very few labels are available (e.g., 1 labeled node per class), GNNs suffer from severe result quality degradation. Several existing studies make an initial effort to ease this situation, but are still far from satisfactory.

In this paper, on few-labeled graph data, we propose an effective framework ABN that is readily applicable to both shallow and deep GNN architectures and significantly boosts classification accuracy. In particular, on a benchmark dataset Cora with only 1 labeled node per class, while the classic graph convolutional network (GCN) only has 44.6% accuracy, an immediate instantiation of ABN over GCN achieves 62.5% accuracy; when applied to a deep architecture DAGNN, ABN improves accuracy from 59.8% to 66.4%, which is state of the art.

ABN obtains superior performance through three main algorithmic designs. First, it selects high-quality unlabeled nodes via an adaptive pseudo labeling technique, so as to adaptively enhance the training process of GNNs. Second, ABN balances the labels of the selected nodes on real-world skewed graph data by pseudo label balancing. Finally, a negative sampling regularizer is designed for ABN to further utilize the unlabeled nodes. The effectiveness of the three techniques in ABN is well-validated by both theoretical and empirical analysis. Extensive experiments, comparing 12 existing approaches on 4 benchmark datasets, demonstrate that ABN achieves state-of-the-art performance.

ACM Reference Format:

Ziang Zhou, Jieming Shi, Shengzhong Zhang, Zengfeng Huang, and Qing Li. 2021. Effective Semi-Supervised Node Classification on Few-Labeled Graph Data. In *Proceedings of SIGKDD '21*. XXXX, 12 pages.

Permission to make digital or hard copies of all or part of this work for personal or classroom use is granted without fee provided that copies are not made or distributed for profit or commercial advantage and that copies bear this notice and the full citation on the first page. Copyrights for components of this work owned by others than ACM must be honored. Abstracting with credit is permitted. To copy otherwise, or republish, to post on servers or to redistribute to lists, requires prior specific permission and/or a fee. Request permissions from permissions@acm.org.

SIGKDD '21,

© 2021 Association for Computing Machinery.
ACM ISBN 978-1-4503-XXXX-X/18/06...\$15.00

1 INTRODUCTION

Graph is an expressive data model, representing objects and the relationships between objects as nodes and edges respectively. Graph data are ubiquitous with a wide range of real-world applications, e.g., social network analysis [28, 37], traffic network prediction [16, 29], protein interface prediction [12], recommendation systems [10, 47]. Among these applications, an important task is to classify the nodes in a graph into various classes. However, one tough situation commonly existing is the lack of labeled data, which are also expensive to collect.

To ease the situation, *semi-supervised node classification* on graphs has attracted much attention from both industry [28, 37] and academia [8, 17, 25, 30, 31, 42]. It aims to leverage a small amount of labeled nodes and additionally a large amount of unlabeled nodes in a graph to train an accurate classifier. Semi-supervised node classification can be framed under the graph-based semi-supervised learning paradigm. Graph convolution networks (GCNs) [24] and their variants [17, 25, 31, 32, 42] are representative solutions under this paradigm. GCNs rely on a message passing scheme called graph convolution that aggregates the neighborhood information of a node, including node features and graph topology, to learn node representations, which can then be used in downstream classification tasks.

Despite the great success of GCNs, under the extreme cases when very few labels are given (e.g., only one labeled node per class), the shallow GCN architecture, typically with two layers [24], cannot effectively propagate the training labels over the input graph, leading to inferior performance. In particular, as shown in our experiments, on a benchmark dataset Cora with 1 labeled node per class, GCN is even less accurate than unsupervised methods, such as DGI [43] and G2G [1]. Recently, several latest studies try to improve accuracy by designing deeper GNNs, e.g., DAGNN and APPNP [25, 31], which also address the over-smoothing issue identified in [5, 30, 46]. However, these deep GNNs are still not directly designed to tackle the scarcity of labeled data, especially when only very few labels are available.

On the other hand, there exist initial efforts to handle insufficient labeled data. Pseudo Labeling [26] assigns a pseudo label to each unlabeled node based on the node's highest probability to belong to a certain class (i.e., confidence) during the training process of GCNs [24]. Self-Training enlarges training set by adding top- K

high-confidence unlabeled nodes [30]. Although these methods can improve the performance, we conduct a thorough analysis with empirical insights in Section 3, revealing that Pseudo Labeling and Self-Training are not adaptive and inflexible to the dynamic changes of confidence scores at different training iterations, and are not able to handle imbalanced labels on real-world skewed graph data.

Facing the challenges of semi-supervised node classification on few-labeled graph data, we propose ABN, an effective framework that is readily applicable to both shallow and deep GNNs, *e.g.*, GCN and DAGNN, and significantly boosts classification accuracy. Figure 1 shows a brief result of ABN applied over GCN and DAGNN, dubbed as ABN_G and ABN_D respectively, when varying the number of labeled nodes per class in $\{1, 3, 5, 10, 20\}$ on Cora dataset. Observe that ABN_G and ABN_D are much more accurate than their respective base GNN models, demonstrating the effectiveness of ABN framework. Specifically, with only 1 labeled node per class, ABN_G achieves 62.5% accuracy while that of GCN is only 44.6%, and compared to DAGNN (59.8%), ABN_D improves accuracy to 66.4%.

ABN achieves superior performance through three main techniques: adaptive pseudo labeling, pseudo label balancing, and negative sampling regularization. Adaptive pseudo labeling selects high-confidence unlabeled nodes according to a confidence distribution per training epoch, so as to adapt to the dynamic training process, and then ABN balances the importance of the selected nodes in gradient descent. Finally, in order to further fully utilize the unlabeled data, a negative sampling regularization technique is designed to enhance the training process. Extensive experiments, using 4 real datasets and comparing against 12 existing solutions, demonstrate that ABN consistently obtains high classification accuracy for semi-supervised node classification on few-labeled graphs.

Summing up, our contributions in this paper are as follows:

- We conduct both empirical and theoretical analysis of semi-supervised node classification problem on graphs with few-labeled nodes, discover important insights, and uncover deficiencies of existing solutions.
- We propose an effective framework ABN with three techniques, namely adaptive pseudo labeling, pseudo label balancing, and negative sampling regularization.
- We apply ABN over both shallow and deep GNN architectures, and achieve state-of-the-art performance.
- We conduct extensive experiments on 4 benchmark datasets and compare ABN with 12 existing solutions, to evaluate the superior performance of ABN.

The rest of the paper is organized as follows. In Section 2, we introduce the semi-supervised node classification problem and explain the most relevant existing solutions. We conduct empirical and theoretical analysis in Section 3, revealing the deficiencies of existing solutions. We present the ABN framework with three techniques in Section 4. Experiments are reported in Section 5. We further review other related work in Section 6. Finally, Section 7 concludes the paper. Appendix consists of proofs and details for reproducibility.

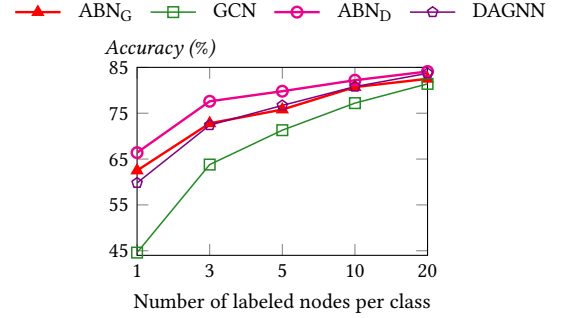


Figure 1: Node classification performance on Cora.

2 PRELIMINARIES

2.1 Problem Formulation

Let $\mathcal{G} = (\mathcal{V}, \mathcal{E}, \mathbf{X})$ be a graph consisting of a node set \mathcal{V} with cardinality n , a set of edges \mathcal{E} of size m , each connecting two nodes in \mathcal{V} , a feature matrix $\mathbf{X} \in \mathbb{R}^{n \times d}$, where d is the number of features in \mathcal{G} . For every node $v_i \in \mathcal{V}$, it has a feature vector $\mathbf{X}_i \in \mathbb{R}^d$, where \mathbf{X}_i is the i -th row of \mathbf{X} . Let c be the number of classes in \mathcal{G} . We use \mathcal{L} to denote the set of labeled nodes, and obviously $\mathcal{L} \subseteq \mathcal{V}$. Let \mathcal{U} be the set of unlabeled nodes and $\mathcal{U} = \mathcal{V} \setminus \mathcal{L}$. Each labeled node $v_i \in \mathcal{L}$ has a one-hot vector $\mathbf{Y}_i \in \{0, 1\}^c$, indicating the class label of v_i . A high-level definition of the semi-supervised node classification problem is as follows.

DEFINITION 1. Given a graph $\mathcal{G} = (\mathcal{V}, \mathcal{E}, \mathbf{X})$, a set of labeled nodes $\mathcal{L} \subseteq \mathcal{V}$, and a class label $\mathbf{Y}_i \in \{0, 1\}^c$ per node $v_i \in \mathcal{L}$, assuming that each node belongs to exactly one class, Semi-Supervised Node Classification predicts the labels of the unlabeled nodes.

In particular, the aim is to leverage the graph \mathcal{G} with the labeled nodes in \mathcal{L} , and to train a forward predicting classification model/function $f(\mathcal{G}, \theta)$ that takes as input the graph \mathcal{G} and a set of trainable parameters θ . The output of f is a matrix $\mathbf{F} \in \mathbb{R}^{n \times c}$, with each i -th row $\mathbf{F}_i \in [0, 1]^c$ representing the output probability vector of node $v_i \in \mathcal{V}$ (the 1-norm of \mathbf{F}_i is normalized to 1). Supposing that $j = \arg \max_{j'} \mathbf{F}_{i,j'}$, we say that, with confidence $\mathbf{F}_{i,j}$, node v_i has class label C_j ; *i.e.*, the largest element $\mathbf{F}_{i,j}$ in vector \mathbf{F}_i is called the *confidence of node v_i* .

We adopt the widely used cross-entropy loss as objective function. For a node v_i , its loss of \mathbf{F}_i with respect to its class label \mathbf{Y}_i , $L(\mathbf{Y}_i, \mathbf{F}_i)$, is defined as follows.

$$L(\mathbf{Y}_i, \mathbf{F}_i) = - \sum_{j=1}^c \mathbf{Y}_{i,j} \ln(\mathbf{F}_{i,j})$$

where $\mathbf{Y}_{i,j}$ is the j -th value in \mathbf{Y}_i and $\mathbf{F}_{i,j}$ is the j -th value in \mathbf{F}_i .

2.2 Related Work

Observe that, in practice, the labeled nodes are few, *i.e.*, $|\mathcal{L}| \ll |\mathcal{U}|$. In literature, there are two directions to address the scarcity of labeled data for semi-supervised node classification: (i) explore multi-hop graph topological features to propagate the labels in \mathcal{L} over the input graph, *e.g.*, GCN [24] and DAGNN [31]; (ii) enhance labeled set \mathcal{L} by Pseudo Labeling [26] or Self-Training [30] over unlabeled set \mathcal{U} . Note that these two directions are not mutually

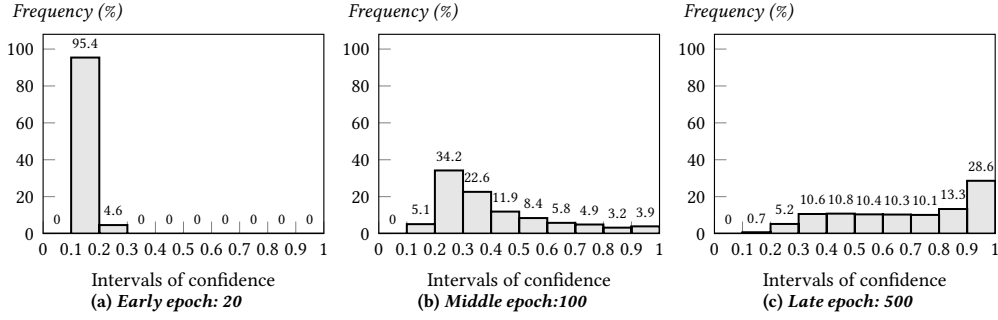


Figure 2: Confidence distributions.

exclusive, but can work together on few-labeled graph data. Here we review the existing studies that are most relevant to this paper.

GCN. GCN [24] is a graph neural network model for semi-supervised classification. GCN learns the representation of each node by iteratively aggregating the representations of its neighbors. Specifically, GCN consists of $k > 0$ layers, each with the same propagation rule defined as follows. At the ℓ -th layer, the hidden representations $\mathbf{H}^{(\ell-1)}$ of previous layer are aggregated to get $\mathbf{H}^{(\ell)}$.

$$\mathbf{H}^{(\ell)} = \sigma(\hat{\mathbf{A}}\mathbf{H}^{(\ell-1)}\mathbf{W}^{(\ell)}), \ell = 1, 2, \dots, k. \quad (1)$$

$\hat{\mathbf{A}} = \tilde{\mathbf{D}}^{-\frac{1}{2}}\tilde{\mathbf{A}}\tilde{\mathbf{D}}^{-\frac{1}{2}}$ is the graph laplacian, where $\tilde{\mathbf{A}} = \mathbf{A} + \mathbf{I}$ is the adjacency matrix of \mathcal{G} after adding self-loops (\mathbf{I} is the identity matrix) and $\tilde{\mathbf{D}}$ is a diagonal matrix with $\tilde{D}_{ii} = \sum_j \tilde{A}_{ij}$. $\mathbf{W}^{(\ell)}$ is a trainable weight matrix of the ℓ -th layer, and σ is a nonlinear activation function. Initially, $\mathbf{H}^{(0)} = \mathbf{X}$. $\mathbf{H}^{(k)}$ is the output \mathbf{F} . Note that GCN usually achieves superior performance with 1-layer or 2-layer models [24]. When applying multiple layers to leverage large receptive fields, the performance degrades severely, due to the over-smoothing issue identified in [5, 30, 46].

DAGNN. A recent deep GNN architecture, DAGNN, tackles the over-smoothing issue and achieves state-of-the-art results by decoupling representation transformation and propagation in GNNs [31]. Then it utilizes an adaptive adjustment mechanism to balance the information from local and global neighborhoods of each node. Specifically, the mathematical expression of DAGNN is as follows. DAGNN uses a learnable parameter $\mathbf{s} \in \mathbb{R}^{c \times 1}$ to adjust the weight of embeddings at different propagation level (from 1 to k).

$$\begin{aligned} \mathbf{Z} &= \text{MLP}(\mathbf{X}) \in \mathbb{R}^{n \times c} \\ \mathbf{H}_\ell &= \hat{\mathbf{A}}^\ell \cdot \mathbf{Z} \in \mathbb{R}^{n \times c}, \ell = 1, 2, \dots, k \\ \mathbf{S}_\ell &= \mathbf{H}_\ell \cdot \mathbf{s} \in \mathbb{R}^{n \times 1}, \ell = 1, 2, \dots, k \\ \hat{\mathbf{S}}_\ell &= [\mathbf{S}_\ell, \mathbf{S}_\ell, \dots, \mathbf{S}_\ell] \in \mathbb{R}^{n \times c}, \ell = 1, 2, \dots, k \\ \mathbf{X}_{out} &= \text{softmax}\left(\sum_{\ell=1}^k \mathbf{H}_\ell \odot \hat{\mathbf{S}}_\ell\right), \end{aligned}$$

where $\hat{\mathbf{A}}^\ell$ is the ℓ -th power of matrix $\hat{\mathbf{A}}$, \odot is the Hadamard product, \cdot is dot product, MLP is the Multilayer Perceptron and softmax operation is on the second dimension.

Pseudo Labeling. Pseudo Labeling assigns to *each* node in \mathcal{U} a pseudo label based on the confidence of node v_i over \mathbf{F}_i [26]. In particular, the pseudo label \tilde{Y}_i of node $v_i \in \mathcal{U}$ is as follows. If $\mathbf{F}_{i,j}$

is the largest element in vector \mathbf{F}_i , $\tilde{Y}_{i,j}$ is 1, otherwise, 0.

$$\tilde{Y}_{i,j} = \begin{cases} 1 & \text{if } j = \arg \max_{j'} \mathbf{F}_{i,j'}, \\ 0 & \text{otherwise,} \end{cases} \quad (2)$$

Then Pseudo Labeling considers a *pseudo loss* L_{pse} that consists of the loss of labeled nodes in \mathcal{L} and the loss of *all* nodes in \mathcal{U} with their pseudo labels as follows.

$$L_{pse} = \frac{1}{|\mathcal{L}|} \cdot \sum_{v_i \in \mathcal{L}} L(\mathbf{Y}_i, \mathbf{F}_i) + \frac{\lambda}{|\mathcal{U}|} \cdot \sum_{v_i \in \mathcal{U}} L(\tilde{\mathbf{Y}}_i, \mathbf{F}_i), \quad (3)$$

where $\lambda \in \mathbb{R}$ is a hyper-parameter controlling the weight of pseudo labels in the loss function.

Self-Training. Self-Training picks the top- K nodes with the highest confidence in \mathcal{U} and adds them with their predicted labels into labeled set \mathcal{L} to extend \mathcal{L} [19, 22, 34, 38, 49]. Then in the following iterations, the classifier will be trained from the extended labeled set. In literature, there are several studies on Self-Training, such as Co-Training which co-trains a GCN with a random walk model [7, 30], M3S [40] which utilizes DeepCluster technique to refine the selected pseudo labels.

3 ANALYSIS

We first conduct an empirical analysis to identify the issues of existing techniques, specifically Pseudo Labeling and Self-Training. Then we theoretically analyze these issues from the perspective of *transductive learning* and *gradient descent*. The analysis motivates the design of our ABN framework in Section 4.

3.1 Empirical Analysis

In the following, we show that (i) Pseudo Labeling and Self-Training are *not adaptive* to the distributions of confidence scores at various training iterations, and (ii) they are not able to handle *imbalanced* pseudo labels on real-world graphs that are often skewed [27]. These issues may degrade the performance of the learned classifier.

In Figures 2a, 2b, and 2c, we illustrate the distributions of the confidence scores of all nodes in unlabeled set \mathcal{U} on Cora with only 1 label per class, at early (20-th), middle (100-th), and late (500-th) epochs, respectively. Observe that the number of high-confidence nodes increases gradually at middle and late epochs as in Figures 2b and 2c. At the early epoch in Figure 2a, 95.4% of the unlabeled nodes are with very low confidence (< 0.2).

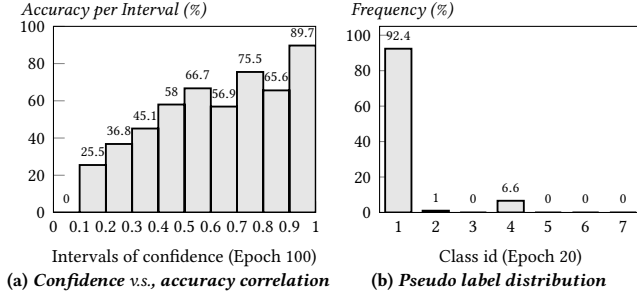


Figure 3: Cora with 1 labeled node per class

First, recall that Pseudo Labeling assigns a label to *every* node v_i in \mathcal{U} , no matter whether the confidence of v_i is actually low or high. This may lead to low-quality training process, at the early epochs when most of the confidence scores are small, which is exactly the case in Figure 2a, where 95.4% of the nodes have confidence below 0.2. Low-quality pseudo labels at early epochs will severely influence the training of later epochs, resulting to unexpected performance degradation. Self-Training, which picks the top- K high-confidence nodes in \mathcal{U} to extend labeled set \mathcal{L} , suffers from the same issue at early epochs. In particular, for a fixed K parameter, at early epochs in Figure 2a, there exist rarely any high-confidence nodes, but Self-Training still has to select top- K nodes even with low confidence. Even worse, in Self-Training, such low-confidence nodes added at early epochs are never moved out from \mathcal{L} [40]. Further, at the 500-th epoch in Figure 2c, when there are 28.6% nodes with 0.9 or even higher confidence, Self-Training with top- K selection may not be able to add all such high-confidence nodes for training.

Second, Figure 3b shows the distribution of the pseudo labels of the nodes in \mathcal{U} at the 20-th epoch on Cora dataset with 7 classes. Obviously the distribution of pseudo labels is highly imbalanced, *i.e.*, 92.4% of the nodes are with class 1 and 6.6% are with class 4. The imbalanced classes (*i.e.*, class 1 in Figure 3b) will heavily affect the direction of gradient descent during the training process. If too many low-confidence nodes are wrongly assigned to a single class at early epochs, Pseudo Labeling and Self-Training will suffer from such imbalanced distribution and result to inferior performance.

3.2 Theoretical Analysis

The semi-supervised node classification problem studied in this paper naturally fits the *transductive learning* setting, since all labeled and unlabeled data in the input graph \mathcal{G} are known and no more new data will be added [9, 24]. In the following, we analyze the problem from the perspective of *gradient descent*, to theoretically explain the issues discovered in Section 3.1.

Under the *ideal case* where we have the labels of *all* nodes in \mathcal{V} (the population), given a classifier $f(\mathcal{G}, \theta)$ with output probability vectors \mathbf{F}_i for all nodes v_i in \mathcal{V} , the population loss L_{pop} is computed as follows. Ideally, the objective is to minimize L_{pop} by evaluating *population gradient* $\nabla_{\theta} L_{pop}$, and find optimal parameters θ^* .

$$L_{pop} = \mathbb{E}_{v_i \sim \mathcal{U}(\mathcal{V})} L(\mathbf{Y}_i, \mathbf{F}_i),$$

where $\mathcal{U}(\mathcal{V})$ is the uniform distribution over node set \mathcal{V} .

However, in practice, due to the scarcity of labeled data (*i.e.*, $|\mathcal{L}| \ll |\mathcal{V}|$), it is impossible to directly evaluate $\nabla_{\theta} L_{pop}$. Therefore, as introduced in Eq. (3), Pseudo Labeling approximates population loss L_{pop} by pseudo loss L_{pse} with the consideration of both labeled nodes and unlabeled nodes (pseudo labels). In other words, it uses *pseudo gradient* $\nabla_{\theta} L_{pse}$ to approximate $\nabla_{\theta} L_{pop}$, so as to minimize the loss, which is a common technique in literature [14, 33].

We rewrite pseudo loss in Eq. (3) as in Eq. (4), and write its gradient $\nabla_{\theta} L_{pse}$ in Eq. (5).

$$L_{pse} = \mathbb{E}_{v_i \sim \mathcal{U}(\mathcal{L})} L(\mathbf{Y}_i, \mathbf{F}_i) + \lambda \cdot \mathbb{E}_{v_i \sim \mathcal{U}(\mathcal{U})} L(\tilde{\mathbf{Y}}_i, \mathbf{F}_i), \quad (4)$$

$$\nabla_{\theta} L_{pse} = \mathbb{E}_{v_i \sim \mathcal{U}(\mathcal{L})} \nabla_{\theta} L(\mathbf{Y}_i, \mathbf{F}_i) + \lambda \cdot \mathbb{E}_{v_i \sim \mathcal{U}(\mathcal{U})} \nabla_{\theta} L(\tilde{\mathbf{Y}}_i, \mathbf{F}_i), \quad (5)$$

where $\mathcal{U}(\mathcal{L})$ and $\mathcal{U}(\mathcal{U})$ are the uniform distributions over labeled node set \mathcal{L} and unlabeled node set \mathcal{U} , respectively.

In a similar way, the population gradient $\nabla_{\theta} L_{pop}$ is as follows. Note that we break \mathcal{V} into \mathcal{L} and \mathcal{U} .

$$\begin{aligned} \nabla_{\theta} L_{pop} &= \mathbb{E}_{v_i \sim \mathcal{U}(\mathcal{V})} \nabla_{\theta} L(\mathbf{Y}_i, \mathbf{F}_i) \\ &= \frac{|\mathcal{L}|}{|\mathcal{V}|} \mathbb{E}_{v_i \sim \mathcal{U}(\mathcal{L})} \nabla_{\theta} L(\mathbf{Y}_i, \mathbf{F}_i) + \frac{|\mathcal{U}|}{|\mathcal{V}|} \mathbb{E}_{v_i \sim \mathcal{U}(\mathcal{U})} \nabla_{\theta} L(\mathbf{Y}_i, \mathbf{F}_i). \end{aligned}$$

Then, we derive a bound of the difference between $\nabla_{\theta} L_{pop}$ and $\nabla_{\theta} L_{pse}$ in Eq. (6). Specifically, let $\lambda = \frac{|\mathcal{U}|}{|\mathcal{L}|}$, and assume that any gradient satisfies a bounded norm (*i.e.*, $\|\nabla_{\theta} L\| \leq \Theta$, for any loss L), which is a common assumption in the analysis of gradient descent [51]. Then the difference between $\nabla_{\theta} L_{pop}$ and $\nabla_{\theta} L_{pse}$ is bounded as follows. The proof of Eq. (6) is in Appendix A.1.

$$\begin{aligned} & \left\| \nabla_{\theta} L_{pse} - \frac{|\mathcal{V}|}{|\mathcal{L}|} \nabla_{\theta} L_{pop} \right\| \\ &= \frac{|\mathcal{U}|}{|\mathcal{L}|} \cdot \left\| \mathbb{E}_{v_i \sim \mathcal{U}(\mathcal{U})} [\nabla_{\theta} L(\tilde{\mathbf{Y}}_i, \mathbf{F}_i) - \nabla_{\theta} L(\mathbf{Y}_i, \mathbf{F}_i)] \right\| \\ &\leq \frac{|\mathcal{U}| \cdot \mathbf{P}_{v_i \sim \mathcal{U}(\mathcal{U})}(\tilde{\mathbf{Y}}_i \neq \mathbf{Y}_i)}{|\mathcal{L}|} \cdot \mathbb{E}_{v_i \sim \mathcal{U}(\mathcal{U})} \left[\left\| \nabla_{\theta} L(\tilde{\mathbf{Y}}_i, \mathbf{F}_i) - \nabla_{\theta} L(\mathbf{Y}_i, \mathbf{F}_i) \right\| \mathbf{1}_{\tilde{\mathbf{Y}}_i \neq \mathbf{Y}_i} \right] \\ &\leq \frac{2\Theta |\mathcal{U}|}{|\mathcal{L}|} \cdot \mathbf{P}_{v_i \sim \mathcal{U}(\mathcal{U})}(\tilde{\mathbf{Y}}_i \neq \mathbf{Y}_i), \end{aligned} \quad (6)$$

where $\mathbf{P}_{v_i \sim \mathcal{U}(\mathcal{U})}(\tilde{\mathbf{Y}}_i \neq \mathbf{Y}_i)$ is the probability that a randomly sampled node $v_i \in \mathcal{U}$ has a wrongly predicted label.

Obviously, $\mathbf{P}_{v_i \sim \mathcal{U}(\mathcal{U})}(\tilde{\mathbf{Y}}_i \neq \mathbf{Y}_i)$ is exactly the classification error on unlabeled set \mathcal{U} . Observe that the bound at the last line in Eq. (6) mainly relies on the quality of pseudo labels $\tilde{\mathbf{Y}}_i$ of nodes v_i in \mathcal{U} . In other words, if we have low-quality pseudo labels from \mathcal{U} , then $\mathbf{P}_{v_i \sim \mathcal{U}(\mathcal{U})}(\tilde{\mathbf{Y}}_i \neq \mathbf{Y}_i)$ tends to be large, leading to a large difference between $\nabla_{\theta} L_{pop}$ and $\nabla_{\theta} L_{pse}$ and consequently resulting to sub-optimal performance. This situation is likely to happen at the early epochs when most nodes have low confidence, but are still assigned with pseudo labels by Pseudo Labeling or chosen by Self-Training, as we have analyzed in Section 3.1. Moreover, at the early epochs when most nodes are with low confidence, the imbalance of pseudo labels may make $\mathbf{P}_{v_i \sim \mathcal{U}(\mathcal{U})}(\tilde{\mathbf{Y}}_i \neq \mathbf{Y}_i)$ even larger, further hampering the training process.

4 THE ABN FRAMEWORK

In this section, we present ABN that addresses the issues identified in Section 3. In a nutshell, ABN develops new gradient formula to be used in the training process and consists of three techniques, namely, adaptive pseudo labeling in Section 4.1, pseudo label balancing in Section 4.2, and negative sampling regularization in Section 4.3. We present the overall ABN framework in Section 4.4.

4.1 Adaptive Pseudo Labeling

First, intuitively, nodes with higher confidence tend to be predicted more accurately, meaning that if a framework selects more nodes with high confidence into the training process, it tends to be more accurate. We verify this assumption in Figure 3a, which shows the *positive* correlation between confidence and accuracy per confidence interval. For each confidence interval (x -axis), we report the percentage of nodes with pseudo labels same as ground-truth labels (y -axis). Second, a new pseudo labeling technique should be adaptive to the evolving of confidence distribution per epoch as shown in Figure 2.

To achieve the above goals, we propose adaptive pseudo labeling that only assigns labels to high-confidence unlabeled nodes per epoch, so as to reduce the effect of $\mathbf{P}_{v_i \sim \mathcal{U}}(\hat{Y}_i \neq Y_i)$ in Eq. (6), instead of assigning pseudo labels to all nodes in \mathcal{U} as Pseudo Labeling does. Specifically, at current epoch, only unlabeled nodes with confidence larger than a threshold β are assigned with an adaptive pseudo label \hat{Y}_i as in Eq. (7). Note that \hat{Y}_i in Eq. (7) and \tilde{Y}_i in Eq. (2) have a simple but vital difference: for any node $v_i \in \mathcal{U}$, \hat{Y}_i can be a zero vector, meaning that v_i has too low confidence ($< \beta$) to earn a label at current epoch, while \tilde{Y}_i always has a 1-element regardless of its confidence. From now on, we refer to \hat{Y}_i as the *adaptive pseudo label* of v_i , and \tilde{Y}_i as the pseudo label of v_i .

$$\hat{Y}_{i,j} = \begin{cases} 1 & \text{if } j = \arg \max_{j'} F_{i,j'} \text{ and } F_{i,j} \geq \beta, \\ 0 & \text{otherwise,} \end{cases} \quad (7)$$

where $\beta \in (0, 1)$ is a confidence threshold.

At *each* epoch, we generate a new adaptive pseudo-labeled set with nonzero \hat{Y}_i , $\mathcal{U}' \subseteq \mathcal{U}$, based on the confidence distribution of current epoch and Eq. (7), to facilitate the computation of pseudo gradient at current epoch. A node that had confidence larger than β in previous epochs is not guaranteed to be in the \mathcal{U}' of current epoch if its confidence is changed below β . Note that there is a trade-off: if β is too large, though the selected nodes are with high confidence, but the number of nodes that contribute to the training process is small; if β is too small, too many low-confidence nodes will be selected into the training process. We experimentally evaluate the choice of β in Section 5.5.

Discussion. Compared with Pseudo Labeling that assigns a pseudo label \tilde{Y}_i to every node v_i in \mathcal{U} regardless of confidence level, we only assign adaptive pseudo labels \hat{Y}_i to nodes with high confidence and generate a new adaptive pseudo-labeled set \mathcal{U}' per epoch. \mathcal{U}' changes in a way adaptive to the confidence distribution per epoch. Each unlabeled node earns its adaptive pseudo label \hat{Y}_i per epoch by its current confidence. But Self-Training has a fixed top- K parameter to add unlabeled nodes into training and never move such nodes out even if they are with low confidence later.

4.2 Pseudo Label Balancing

Figure 3b illustrates pseudo label imbalance at early epochs. Initially, while the confidence of all unlabeled nodes are low (shown in Figure 2a), if too many unlabeled nodes are rashly assigned to a class, this will severely influence the search direction of gradient descent.

Inspired by classic class-reweight techniques [18, 21], we design a pseudo label balancing technique to ease the situation. In a nutshell, at each epoch, after pseudo labeling by Eq. (2), if a pseudo-labeled node v_i belongs to a class with N_i pseudo-labeled nodes, we reduce the importance of v_i in gradient descent by a factor of $\frac{1}{N_i}$. Specifically, the pseudo gradient update formula by considering adaptive pseudo labeling and pseudo label balancing is in Eq. (8). Compared with Eq. (5) of Pseudo Labeling, there are two differences: (i) we use adaptive pseudo labels in \mathcal{U}' rather than \mathcal{U} , and (ii) we consider pseudo label balancing $\frac{1}{N_i}$ per node $v_i \in \mathcal{U}'$.

$$\nabla_{\theta} L_{pse} = \frac{1}{|\mathcal{L}|} \cdot \sum_{\forall v_i \in \mathcal{L}} \nabla_{\theta} L(Y_i, F_i) + \lambda \cdot \sum_{\forall v_i \in \mathcal{U}'} \frac{1}{N_i} \cdot \nabla_{\theta} L(\hat{Y}_i, F_i). \quad (8)$$

4.3 Negative Sampling Regularization

Under extreme cases with very few labeled nodes (*e.g.*, 1 labeled node per class), we further design a negative sampling regularization technique to utilize the input graph for training. Negative sampling is widely used in unsupervised learning, such as network embedding [48]. Intuitively, the embedding of a node v should be distant to the embedding of another node u if these two nodes are faraway on the input graph \mathcal{G} [43, 48].

For semi-supervised node classification, we apply negative sampling over labels instead of embeddings. Specifically, a positive sample is a node v_i in \mathcal{L} or \mathcal{U}' . We sample a set \mathcal{I} of positive samples from $\mathcal{L} \cup \mathcal{U}'$ uniformly at random. The negative samples of a positive sample v_i are the nodes that are not directly connected to v_i in graph \mathcal{G} . For *each* positive sample v_i in \mathcal{I} , we sample a fixed-size set \mathcal{J}_i of negative samples uniformly at random.

For a positive-negative pair (v_i, v_j) , compared with the Y_i (or \hat{Y}_i) of $v_i \in \mathcal{L} \cup \mathcal{U}'$, the intention is to let the output vector F_j of v_j to be as different as possible. Here, without ambiguity, we abuse the symbol \hat{Y}_i and use it to represent the adaptive pseudo label or ground-truth label of node $v_i \in \mathcal{L} \cup \mathcal{U}'$. Denote $\mathbf{1}$ as the all-one vector in \mathbb{R}^c . Then we have the following loss of all positive-negative pairs.

$$L_{neg} = \frac{1}{|\mathcal{I}| \cdot |\mathcal{J}_i|} \sum_{\forall v_i \in \mathcal{I}} \sum_{\forall v_j \in \mathcal{J}_i} L(\hat{Y}_i, \mathbf{1} - F_j) \quad (9)$$

4.4 Put Things Together

In summary, by Eq. (8) and Eq. (9), we compute the following pseudo gradient per epoch and use it to optimize the training process.

$$\begin{aligned} \nabla_{\theta} L_{pse} &= \frac{1}{|\mathcal{L}|} \cdot \sum_{\forall v_i \in \mathcal{L}} \nabla_{\theta} L(Y_i, F_i) + \lambda \cdot \sum_{\forall v_i \in \mathcal{U}'} \frac{1}{N_i} \cdot \nabla_{\theta} L(\hat{Y}_i, F_i) \\ &+ \frac{\lambda_1}{|\mathcal{I}| \cdot |\mathcal{J}_i|} \sum_{\forall v_i \in \mathcal{I}} \sum_{\forall v_j \in \mathcal{J}_i} \nabla_{\theta} L(\hat{Y}_i, \mathbf{1} - F_j), \end{aligned} \quad (10)$$

Algorithm 1: ABN Framework Over GNNs

```

1 Input: Graph  $\mathcal{G} = (\mathcal{V}, \mathcal{E}, \mathbf{X})$  with labeled node set  $\mathcal{L}$  and
  unlabeled node set  $\mathcal{U}$ 
2 Output: the learned classifier  $f(\cdot, \theta)$ .
3 Generate initial parameter  $\theta$  for model  $f(\cdot, \cdot)$ .
4 for each epoch  $t = 0, 1, 2, \dots, T$  do
5   Use GNN to compute prediction  $\mathbf{F} \leftarrow f(\mathcal{G}, \theta)$ 
6   Get adaptive pseudo-labeled set  $\mathcal{U}'$  (Section 4.1)
7   Get balancing factor  $\frac{1}{N_i}$  per node  $v_i \in \mathcal{U}'$  (Section 4.2)
8   Negative sampling using  $\mathcal{L} \cup \mathcal{U}'$  and  $\mathcal{G}$  (Section 4.3)
9   Get  $\nabla_{\theta^t} L_{pse}$  of current epoch by Eq. (10) (Section 4.4)
10  Update model parameters by
     $\theta \leftarrow \text{Adam Optimizer}(\theta, \text{gradient} = \nabla_{\theta} L_{pse})$ .
11  if Convergence then
12    Break
13  end
14 end

```

where λ_1 is a factor controlling the weight of negative sampling.

Algorithm 1 summarizes the pseudo-code of ABN over GNNs, and it takes as input a graph \mathcal{G} with labeled nodes \mathcal{L} and unlabeled nodes \mathcal{U} . Note that ABN can be instantiated over either a shallow or a deep GNN, *e.g.*, GCN and DAGNN introduced in Section 2.2. The output of Algorithm 1 is the learned classification model f with trainable parameters θ . At Line 3, ABN initializes the trainable parameters θ by Xavier [13]. Then from Lines 4 to 14, ABN trains the classification model per epoch t iteratively, until convergence or the max number T of iterations is reached. Specifically, at Line 5, ABN first use a GNN to obtain the forward prediction output \mathbf{F} . Then (Line 6) ABN detects the adaptive pseudo-labeled set \mathcal{U}' and assigns pseudo labels to these nodes by Eq. (7). Next (Line 7), we obtain the pseudo label balancing factor $\frac{1}{N_i}$ of each node v_i in \mathcal{U}' , after which, at Line 8 we perform negative sampling to obtain \mathcal{I} and \mathcal{J}_i . At Line 9, ABN computes the gradient $\nabla_{\theta^t} L_{pse}$ of current epoch according to Eq. (10). And at Line 10, ABN updates model parameters θ for next epoch by Adam optimizer [23] over $\nabla_{\theta^t} L_{pse}$.

5 EXPERIMENTS

We experimentally evaluate ABN on GNNs against 12 competitors for semi-supervised node classification on 4 real-world benchmark graph datasets. All experiments are conducted on a machine powered by an Intel(R) Xeon(R) E5-2603 v4 @ 1.70GHz CPU, 131GB RAM, 16.04.1-Ubuntu, and 4 Nvidia Geforce 1080ti Cards with Cuda version 10.2. Source codes of all competitors are obtained from the respective authors. Our ABN framework is implemented in Python, using libraries including PyTorch [35] and PyTorch Geometric [11]. An anonymous link of our source code is provided in Appendix B. Apart from the descriptions in this section, we explain more details on reproducibility in Appendix B.

5.1 Datasets and Competitors

Datasets. Table 2 shows the statistics of the 4 real-world graphs used in our experiments. We list the number of nodes, edges, features and classes in each graph dataset respectively. Specifically, the 4 datasets are Cora [39], Citeseer [39], Pubmed [39], and Corefull [1], all of which are widely used for benchmarking node classification performance in existing studies [30, 31, 40]. Notice that every node in these graphs has a ground-truth class label.

Competitors. We compare with 12 existing solutions, including LP (Label Propagation) [45], DeepWalk [36], LINE [41], G2G [1], DGI [43], GCN [24], GAT [42], MoNet [32], APPNP [25], DAGNN [31], STs (Self-Training and its variants) [30], and PL (Pseudo Labeling [26] on GCN). In particular, GCN, GAT, MoNet, APPNP, and DAGNN are GNNs with either shallow or deep architectures. DeepWalk, DGI, LINE, and G2G are unsupervised network embedding methods. STs represents the four variants over GCN in [30], including Self-Training, Co-Training, Union, and Intersection; we summarize the best results among these four variants as the results of STs. Remark that there are other existing solutions, such as M3S [40], but their codes are not available yet when this paper is submitted, and thus these solutions are not compared.

5.2 Experimental Settings

We evaluate our framework and the competitors on semi-supervised node classification tasks with various settings. In particular, for each graph dataset, we repeat experiments on 100 random data splits as suggested in [30, 31] and report the average performance. For each graph dataset, we vary the number of labeled nodes per class in $\{1, 3, 5, 10, 20\}$. Now we explain what a random data split is. For example, when the number of labeled nodes per class on Cora is 3 (denoted as Cora-3), since Cora has 7 classes, we randomly pick 3 nodes per class, combining together as a training set of size 21 (*i.e.*, the labeled node set \mathcal{L}), and then, among the remaining nodes, we randomly select 500 nodes as a validation set, and 1000 nodes as a test set, following convention in existing work [31]. Each data split consists of a training set, a validation set, and a test set as mentioned above. Table 1 summarizes the size of training, validation, test sets and corresponding label rate of all datasets.

We use the classification accuracy on test set as evaluation metric. Specifically, accuracy is defined as the fraction of the testing nodes whose class labels are correctly predicted by the learned classifier.

5.3 Implementation Details

Competitors. We use the parameters suggested in the original papers of the competitors to tune their models under various classification task settings explained in Section 5.2, and report the best results of the competitors. Notice that for unsupervised network embedding methods, including DeepWalk, DGI, LINE, and G2G, after obtaining the embedding results, we use logistic regression to train a node classifier over the embedding results [1, 43].

ABN over GCN and DAGNN. We instantiate ABN framework over the classic GCN model with 2 layers and a recent deep GNN architecture DAGNN to demonstrate the effectiveness and applicability of ABN. The instantiation of ABN over GCN and DAGNN are dubbed as ABN_G and ABN_D respectively for brevity. ABN_G and

Table 1: Summary of data splits under various settings of all datasets.

Dataset	Cora					CiteSeer					PubMed					Cora-full				
# labels per class	1	3	5	10	20	1	3	5	10	20	1	3	5	10	20	1	3	5	10	20
# of Classes	7					6					3					67				
Training set size	7	21	35	70	140	6	18	30	60	120	3	9	15	30	60	67	201	335	670	1340
Validation set size	500	500	500	500	500	500	500	500	500	500	500	500	500	500	500	500	500	500	500	500
Test set size	1000	1000	1000	1000	1000	1000	1000	1000	1000	1000	1000	1000	1000	1000	1000	1000	1000	1000	1000	1000
Label rate	0.25%	0.75%	1.25%	2.51%	5.01%	0.18%	0.54%	0.90%	1.81%	3.61%	0.02%	0.05%	0.07%	0.15%	0.3%	0.36%	1.07%	1.79%	3.69%	7.16%

Table 2: Datasets

	Cora	Citeseer	Pubmed	Cora-full
# of Nodes	2708	3327	19717	19793
# of Edges	5429	4732	44338	65311
# of Features	1433	3703	500	8710
# of Classes	7	6	3	67

ABN_D has parameters (i) inherited from GCN and DAGNN and (ii) developed in ABN. Hence, we first tune the best parameters of the base models under each classification task setting on each dataset. After obtaining the best parameters of the base models, we then tune ABN_G and ABN_D for adaptive pseudo labeling parameter β in range $[0, 1]$, and its weight λ in $\{0.1, 1\}$, pseudo label balancing enabler in $\{\text{True}, \text{False}\}$, negative sampling regularization weight λ_1 in $\{0, 0.1, 0.3, 1, 3\}$, and the number of positive samples and the number of negative samples per positive sample in $\{(1, 10), (2, 5), (5, 2), (10, 1)\}$. The best parameters of each task setting are in Appendix B as well as in the submitted source code.

5.4 Overall Results

Table 3 reports the classification accuracy (in percentage) of all methods on CiteSeer and Cora, when varying the number of labeled nodes per class in $\{1, 3, 5, 10, 20\}$. For each classification task, the best (*i.e.*, highest) accuracy is in bold, and the second and third best accuracy are underlined.

An overall observation is that ABN_G and ABN_D consistently outperform their respective base GNN models, *i.e.*, GCN and DAGNN respectively, by a significant margin under all settings on both CiteSeer and Cora, and they achieve state-of-the-art performance. This demonstrates the power of the proposed ABN framework to boost classification performance. In particular, on the left side of Table 3 (CiteSeer), ABN_G consistently achieves the highest accuracy under all settings, compared with all competitors. For instance, on CiteSeer-1 with only 1 labeled node per class, ABN_G has 56.2% accuracy, while the best competitor DAGNN only achieves 46.5% accuracy. Further, ABN_G outperforms GCN that has 40.4% on CiteSeer-1 by 15.8%. Moreover, ABN_D is always the second best performer among all methods on CiteSeer dataset. Similarly, on the right side of Table 3 (Cora), ABN_D achieves the best accuracy under all classification task settings. For instance, on Cora-1, ABN_G improves GCN from 44.6% to 62.5% (*i.e.*, 17.9% improvement), and ABN_D has 66.4% accuracy, outperforming DAGNN that has 59.8% accuracy by a significant margin.

Table 3: Accuracy results (in percentage) on CiteSeer and Cora respectively, averaged over 100 random data splits. (The best accuracy is in bold, second and third are underlined.)

# of Labels per class	CiteSeer					Cora				
	1	3	5	10	20	1	3	5	10	20
LP	30.1	37.0	39.3	41.9	44.8	51.5	60.5	62.5	64.2	67.3
DeepWalk	28.3	34.7	38.1	42.0	45.6	40.4	53.8	59.4	65.4	69.9
LINE	28.0	34.7	38.0	43.1	48.5	49.4	62.6	63.4	71.1	74.0
G2G	45.1	56.4	60.3	63.1	65.7	54.5	68.1	70.9	73.8	75.8
DGI	46.1	<u>59.2</u>	<u>64.1</u>	67.6	68.7	55.3	70.9	72.6	76.4	77.9
STs	37.2	51.8	60.7	67.4	70.2	53.1	67.3	72.5	76.2	79.8
PL	15.3	17.3	18.1	17.7	28.2	15.2	18.2	20.4	63.5	<u>83.1</u>
GAT	32.8	48.6	54.9	60.8	68.2	41.8	61.7	71.1	76.0	79.6
MoNet	38.8	52.9	59.7	64.6	66.9	43.4	61.2	70.9	76.1	79.3
APPNP	34.6	52.2	59.4	66.0	<u>71.8</u>	44.7	66.3	74.1	79.0	81.9
DAGNN	<u>46.5</u>	58.8	63.6	<u>67.9</u>	71.2	<u>59.8</u>	<u>72.4</u>	<u>76.7</u>	<u>80.8</u>	<u>83.7</u>
GCN	40.4	53.5	61.0	65.8	69.5	44.6	63.8	71.3	77.2	81.4
ABN_G	56.2	66.4	68.0	70.2	72.1	<u>62.5</u>	<u>72.8</u>	<u>75.8</u>	<u>80.7</u>	82.5
ABN_D	<u>48.5</u>	<u>65.9</u>	<u>67.9</u>	<u>69.8</u>	72.1	66.4	77.6	79.8	82.2	84.1

Apart from the superior performance of our ABN framework, in Table 3, we can observe three interesting findings. First, under extremely-few-labels settings (*e.g.*, CiteSeer-3), unsupervised methods G2G (56.4%) and DGI (59.2%) achieve better performance than GNNs, *e.g.*, GCN (53.5%) and DAGNN (58.8%). One reason is that the unsupervised methods are good at cases when no labeled data are available, while GNNs still require a sufficient amount of labeled data. This finding demonstrates the intuition of the negative sampling regularization technique in Section 4.3, and also sheds light on possible future research directions to use unsupervised techniques to further enhance the performance of semi-supervised learning. Second, PL (Pseudo Labeling in Section 2.2) has low accuracy as reported in Table 3, validating our analysis of its potential issues in Section 3. Third, the performance gap between our methods and competitors enlarges as the number of labels per class decreases, which further illustrates the effectiveness of the proposed ABN framework under extreme settings on graphs with very few-labeled nodes per class.

Table 4 presents the classification accuracy of all methods under all settings in $\{1, 3, 5, 10, 20\}$ on PubMed and Cora-full datasets. We exclude from this table, the inaccurate competitors (*e.g.*, DeepWalk and LINE) that are obviously outperformed by other competitors. Observe that on PubMed and Cora-full, ABN_D and ABN_G achieve either the highest accuracy in bold or top-3 accuracy underlined.

Table 4: Accuracy results (in percentage) on PubMed and Cora-full respectively, averaged over 100 random data splits. (The best accuracy is in bold, second and third are underlined.)

# of Labels per class	PubMed					Cora-full				
	1	3	5	10	20	1	3	5	10	20
LP	55.7	61.9	63.5	65.2	66.4	26.3	32.4	35.1	38.0	41.0
G2G	55.2	64.5	67.4	72.0	74.3	25.8	36.4	43.3	49.3	54.3
DGI	55.1	63.4	65.3	71.8	73.9	26.2	37.9	46.5	55.3	59.8
STs	55.1	65.4	69.7	74.0	78.5	<u>29.2</u>	<u>43.6</u>	48.9	53.4	<u>60.8</u>
PL	34.9	35.1	49.2	49.9	77.5	23.5	19.1	24.2	31.3	57.9
APPNP	54.8	66.9	70.8	76.0	<u>79.4</u>	24.3	41.5	48.5	55.3	60.1
DAGNN	<u>59.4</u>	<u>69.5</u>	<u>72.0</u>	<u>76.8</u>	<u>80.1</u>	27.3	43.2	<u>49.8</u>	<u>55.8</u>	60.4
GCN	55.5	66.0	70.4	74.6	78.7	24.5	41.4	48.1	<u>55.8</u>	60.2
ABN _G	<u>60.8</u>	<u>67.8</u>	<u>71.6</u>	<u>76.1</u>	<u>79.4</u>	30.8	44.9	<u>49.4</u>	<u>56.6</u>	<u>60.9</u>
ABN _D	61.0	72.1	74.9	78.2	80.6	<u>27.6</u>	<u>44.4</u>	51.1	56.8	61.2

Also, ABN_G and ABN_D are consistently better than their base GNN models GCN and DAGNN respectively. For instance, on PubMed-1, ABN_G achieves 60.8% accuracy, 5.3% better than GCN; ABN_D has 61.0% accuracy while that of DAGNN is 59.4%.

In summary, the experimental results presented in Tables 3 and 4 validate the effectiveness of the proposed ABN framework to boost classification performance under the graph-based semi-supervised learning paradigm.

5.5 Ablation Study and Parameter Evaluation

Ablation Study. We conduct ablation study to evaluate the contributions of the three techniques of ABN presented in Section 4. Denote (i) ABN as the framework with all techniques enabled, (ii) ABN-N as ABN excluding negative sampling regularization in Section 4.3, and (iii) ABN-N-B as ABN excluding both pseudo label balancing in Section 4.2 and negative sampling regularization. In other words, ABN-N-B is the method with *only* adaptive pseudo labeling enabled (Section 4.1).

Figures 4a and 4b report the ablation results of ABN_G and ABN_D respectively, on Cora when varying the number of labels per class. Observe that the accuracy indeed improves significantly when adding pseudo label balancing and negative sampling regularization one after another. Moreover, comparing ABN_G-N-B in Figure 4a with the results of PL (Pseudo Labeling on GCN) on Cora in Table 3, it is easy to see that ABN_G-N-B outperforms PL by a significant margin, demonstrating the effectiveness of adaptive pseudo labeling technique presented in Section 4.1. For example, on Cora-3, ABN_G-N-B has 45.2% accuracy (Figure 4a) while that of PL is just 18.2% in Table 3. The ablation study on ABN_D in Figure 4b yields the same observations and indicates the effectiveness of the three techniques in ABN framework. In addition, one may observe that ABN-N is slightly better than ABN when the number of labels per class is 10 and 20 in Figure 4a. The reason is that, on Cora-10 and Cora-20, there are enough labels for semi-supervised training. Thus, in Eq. (10), there is a λ_1 parameter to limit the importance of negative sampling regularization when there are sufficient labels.

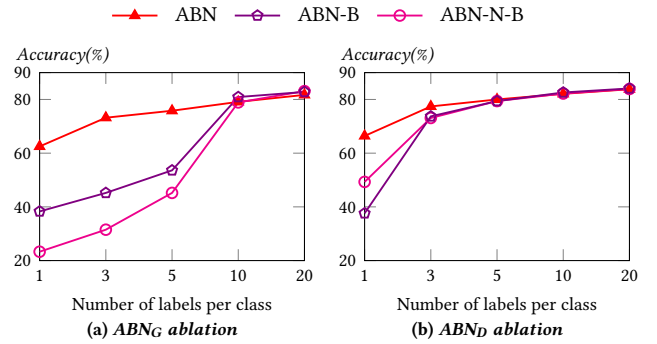


Figure 4: Ablation study of ABN on Cora.

Parameter Evaluation. As mentioned in Section 4.1, there exists a trade-off on the choice of β . Here we report the results when varying β from 0.1 to 0.9 with step 0.1, on Cora-1, Cora-3, and Cora-5 in Figure 5. Observe that, as β increases, especially on Cora-1, the accuracy increases gradually to a peak and then drops, illustrating the trade-off of β in adaptive pseudo labeling. Also when there are more labels, *e.g.*, Cora-5, the performance is relatively stable. Nevertheless, the results in Figure 5 demonstrate that adaptive pseudo labeling is effective when β is fine-tuned on each classification task of each dataset.

6 OTHER RELATED WORK

We review other related work here, excluding GCN [24], DAGNN [31], Pseudo Labeling [26], and Self-Training [30] that are already explained in Section 2.2.

Graph Neural Networks. Apart from GCN and DAGNN, in literature, there exist many other GNN variants, to leverage graph topology and node features for graph representation learning and downstream tasks. Initial studies apply convolution operation in the spectral domain, where the eigenvectors of the graph Laplacian are considered as the Fourier basis [3, 8, 20]. Then GAT [42] assigns different weights to nodes in the same neighborhood via attention mechanisms. MoNet [32] defines convolutions directly in the spatial domain using mixture model CNNs. The above GNNs are with shallow architecture. There are many deep GNNs proposed, *e.g.*, DAGNN and others in [6, 25, 31]. For instance, APPNP [25] proposes a propagation rule based on personalized PageRank [2], so as to gather both local and global information on graphs. However, as evaluated in our experiments, these methods still have space for improvement since they are not directly designed to tackle the scarcity of labeled data.

Network Embedding. Network embedding aims to learn a low-dimensional embedding vector per node in an unsupervised manner. The learned embedding vectors can be then used in downstream tasks, including node classification. There exists a collection of network embedding solutions, *e.g.*, [1, 15, 36, 41, 44]. DeepWalk uses truncated random walks to learn latent representations, with the assumption that nodes are similar if they are close by random walks [36]. LINE preserves and concatenates the first-order and second-order proximity representations between nodes [41]. G2G [1] embeds each node as a Gaussian distribution according to a novel ranking similarity based on the shortest path distances

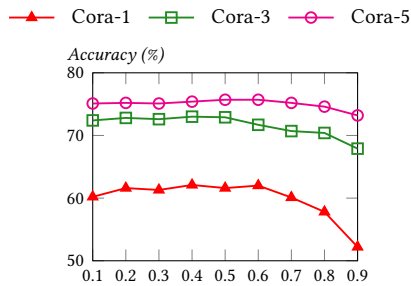


Figure 5: Accuracy v.s., varying β

between nodes. DGI [43] is an embedding method based on GCNs with unsupervised objective that is to maximize mutual information between patch representations and corresponding high-level summaries of graphs. However, these unsupervised methods do not leverage labeled data at all, and thus are not as accurate as our methods as evaluated in experiments.

Orthogonal Self-training Studies. Self-training itself is a general methodology [22] and is used in various domains in addition to graph data. It is used in word-sense disambiguation [19, 49], bootstrap for information extraction and learning subjective nouns [38], and text classification [34]. In [50], it suggests that selecting informative unlabeled data using a guided search algorithm can significantly improve performance over standard self-training framework. Buchnik and Cohen [4] mainly consider self-training for diffusion-based techniques. The above self-training studies focus on either different data domains, e.g., images and texts, or different problems, and thus are orthogonal to our work.

7 CONCLUSION

This paper presents ABN, an effective framework for semi-supervised node classification on few-labeled graph data. ABN achieves superior performance on graphs with extremely few labeled nodes, through three main designs: adaptive pseudo labeling that adaptively selects high-confidence unlabeled nodes based on the confidence distribution of current epoch to enhance training process, pseudo label balancing that handles label imbalance in real-world skewed graph data, and negative sampling regularization that further fully utilizes unlabeled data to train a high-quality classifier. The effectiveness of ABN is extensively evaluated on 4 real graphs, compared against 12 existing solutions. Regarding future work, we plan to enhance ABN by investigating other unsupervised techniques, and also implement ABN on top of more GNN architectures to further demonstrate its applicability.

REFERENCES

- [1] Aleksandar Bojchevski and Stephan Günnemann. 2018. Deep Gaussian Embedding of Graphs: Unsupervised Inductive Learning via Ranking. In *ICLR*.
- [2] Sergey Brin and Lawrence Page. 1998. The Anatomy of a Large-Scale Hypertextual Web Search Engine. *Comput. Networks* (1998), 107–117.
- [3] Joan Bruna, Wojciech Zaremba, Arthur Szlam, and Yann LeCun. 2014. Spectral Networks and Locally Connected Networks on Graphs. In *ICLR*.
- [4] Eliav Buchnik and Edith Cohen. 2018. Bootstrapped graph diffusions: Exposing the power of nonlinearity. In *Abstracts of the 2018 ACM International Conference on Measurement and Modeling of Computer Systems*. 8–10.
- [5] Deli Chen, Yankai Lin, Wei Li, Peng Li, Jie Zhou, and Xu Sun. 2020. Measuring and Relieving the Over-Smoothing Problem for Graph Neural Networks from the Topological View. In *AAAI*. 3438–3445.
- [6] Ming Chen, Zhewei Wei, Zengfeng Huang, Bolin Ding, and Yaliang Li. 2020. Simple and Deep Graph Convolutional Networks. In *ICML*. 1725–1735.
- [7] Minmin Chen, Kilian Q. Weinberger, and John Blitzer. 2011. Co-Training for Domain Adaptation. In *NeurIPS*. 2456–2464.
- [8] Michaël Defferrard, Xavier Bresson, and Pierre Vandergheynst. 2016. Convolutional Neural Networks on Graphs with Fast Localized Spectral Filtering. In *NeurIPS*. 3837–3845.
- [9] Ran El-Yaniv and Dmitry Pechyony. 2007. Transductive Rademacher Complexity and Its Applications. In *COLT*. 157–171.
- [10] Wenqi Fan, Yao Ma, Qing Li, Yuan He, Yihong Eric Zhao, Jiliang Tang, and Dawei Yin. 2019. Graph Neural Networks for Social Recommendation. In *WWW*. 417–426.
- [11] Matthias Fey and Jan Eric Lenssen. 2019. Fast graph representation learning with PyTorch Geometric. *arXiv preprint arXiv:1903.02428* (2019).
- [12] Alex Fout, Jonathon Byrd, Basir Shariat, and Asa Ben-Hur. 2017. Protein Interface Prediction using Graph Convolutional Networks. In *NeurIPS*. 6530–6539.
- [13] Xavier Glorot and Yoshua Bengio. 2010. Understanding the difficulty of training deep feedforward neural networks. In *AISTATS*. 249–256.
- [14] Robert Mansel Gower, Nicolas Loizou, Xun Qian, Alibek Sailanbayev, Egor Shulgin, and Peter Richtárik. 2019. SGD: General analysis and improved rates. In *International Conference on Machine Learning*. PMLR, 5200–5209.
- [15] Aditya Grover and Jure Leskovec. 2016. node2vec: Scalable Feature Learning for Networks. In *SIGKDD*. 855–864.
- [16] Shengnan Guo, Youfang Lin, Ning Feng, Chao Song, and Huaiyu Wan. 2019. Attention Based Spatial-Temporal Graph Convolutional Networks for Traffic Flow Forecasting. In *AAAI*. 922–929.
- [17] William L. Hamilton, Zitao Ying, and Jure Leskovec. 2017. Inductive Representation Learning on Large Graphs. In *NeurIPS*. 1024–1034.
- [18] Haibo He and Edwardo A. Garcia. 2009. Learning from Imbalanced Data. *IEEE Trans. Knowl. Data Eng.* (2009), 1263–1284.
- [19] Marti Hearst. 1991. Noun homograph disambiguation using local context in large text corpora. *Using Corpora* (1991), 185–188.
- [20] Mikael Henaff, Joan Bruna, and Yann LeCun. 2015. Deep convolutional networks on graph-structured data. *arXiv preprint arXiv:1506.05163* (2015).
- [21] Chen Huang, Yining Li, Chen Change Loy, and Xiaoou Tang. 2016. Learning Deep Representation for Imbalanced Classification. In *CVPR*. 5375–5384.
- [22] H. J. Scudder III. 1965. Probability of error of some adaptive pattern-recognition machines. *IEEE Trans. Inf. Theory* (1965), 363–371.
- [23] Diederik P. Kingma and Jimmy Ba. 2015. Adam: A Method for Stochastic Optimization. In *ICLR*.
- [24] Thomas N. Kipf and Max Welling. 2017. Semi-Supervised Classification with Graph Convolutional Networks. In *ICLR*.
- [25] Johannes Klicpera, Aleksandar Bojchevski, and Stephan Günnemann. 2019. Predict then Propagate: Graph Neural Networks meet Personalized PageRank. In *ICLR*.
- [26] Dong-Hyun Lee. 2013. Pseudo-label: The simple and efficient semi-supervised learning method for deep neural networks. In *Workshop on Challenges in Representation Learning, ICML*.
- [27] Jure Leskovec, Jon M. Kleinberg, and Christos Faloutsos. 2005. Graphs over time: densification laws, shrinking diameters and possible explanations. In *SIGKDD*. 177–187.
- [28] Chang Li and Dan Goldwasser. 2019. Encoding Social Information with Graph Convolutional Networks for Political Perspective Detection in News Media. In *ACL*. 2594–2604.
- [29] Jia Li, Zhichao Han, Hong Cheng, Jiao Su, Pengyun Wang, Jianfeng Zhang, and Lujia Pan. 2019. Predicting Path Failure In Time-Evolving Graphs. In *SIGKDD*. 1279–1289.
- [30] Qimai Li, Zhichao Han, and Xiao-Ming Wu. 2018. Deeper Insights Into Graph Convolutional Networks for Semi-Supervised Learning. In *AAAI*. 3538–3545.
- [31] Meng Liu, Hongyang Gao, and Shuiwang Ji. 2020. Towards Deeper Graph Neural Networks. In *SIGKDD*. 338–348.
- [32] Federico Monti, Davide Boscaini, Jonathan Masci, Emanuele Rodolà, Jan Svoboda, and Michael M. Bronstein. 2017. Geometric Deep Learning on Graphs and Manifolds Using Mixture Model CNNs. In *CVPR*. 5425–5434.
- [33] Yurii E. Nesterov and Vladimir G. Spokoiny. 2017. Random Gradient-Free Minimization of Convex Functions. *Found. Comput. Math.* (2017), 527–566.
- [34] Kamal Nigam, Andrew McCallum, Sebastian Thrun, and Tom M. Mitchell. 2000. Text Classification from Labeled and Unlabeled Documents using EM. *Mach. Learn.* (2000), 103–134.
- [35] Adam Paszke, Sam Gross, Francisco Massa, Adam Lerer, James Bradbury, Gregory Chanan, Trevor Killeen, Zeming Lin, Natalia Gimelshein, Luca Antiga, Alban Desmaison, Andreas Köpf, Edward Yang, Zachary DeVito, Martin Raison, Alykhan Tejani, Sasank Chilamkurthy, Benoit Steiner, Lu Fang, Junjie Bai, and Soumith Chintala. 2019. PyTorch: An Imperative Style, High-Performance Deep Learning Library. In *NeurIPS*. 8024–8035.
- [36] Bryan Perozzi, Rami Al-Rfou, and Steven Skiena. 2014. DeepWalk: online learning of social representations. In *SIGKDD*. 701–710.

- [37] Jiezhong Qiu, Jian Tang, Hao Ma, Yuxiao Dong, Kuansan Wang, and Jie Tang. 2018. DeepInf: Social Influence Prediction with Deep Learning. In *SIGKDD*. 2110–2119.
- [38] Ellen Riloff and Rosie Jones. 1999. Learning Dictionaries for Information Extraction by Multi-Level Bootstrapping. In *AAAI*. 474–479.
- [39] Prithviraj Sen, Galileo Namata, Mustafa Bilgic, Lise Getoor, Brian Gallagher, and Tina Eliassi-Rad. 2008. Collective Classification in Network Data. *AI Mag.* (2008), 93–106.
- [40] Ke Sun, Zhouchen Lin, and Zhanxing Zhu. 2020. Multi-Stage Self-Supervised Learning for Graph Convolutional Networks on Graphs with Few Labeled Nodes. In *AAAI*. 5892–5899.
- [41] Jian Tang, Meng Qu, Mingzhe Wang, Ming Zhang, Jun Yan, and Qiaozhu Mei. 2015. LINE: Large-scale Information Network Embedding. In *WWW*. 1067–1077.
- [42] Petar Velickovic, Guillem Cucurull, Arantxa Casanova, Adriana Romero, Pietro Liò, and Yoshua Bengio. 2018. Graph Attention Networks. In *ICLR*.
- [43] Petar Velickovic, William Fedus, William L. Hamilton, Pietro Liò, Yoshua Bengio, and R. Devon Hjelm. 2019. Deep Graph Infomax. In *ICLR*.
- [44] Daixin Wang, Peng Cui, and Wenwu Zhu. 2016. Structural Deep Network Embedding. In *SIGKDD*. 1225–1234.
- [45] Xiao-Ming Wu, Zhenguo Li, Anthony Man-Cho So, John Wright, and Shih-Fu Chang. 2012. Learning with Partially Absorbing Random Walks. In *NeurIPS*. 3086–3094.
- [46] Keyulu Xu, Chengtao Li, Yonglong Tian, Tomohiro Sonobe, Ken-ichi Kawarabayashi, and Stefanie Jegelka. 2018. Representation Learning on Graphs with Jumping Knowledge Networks. In *ICML*. 5449–5458.
- [47] Gang Yang, Xiaofeng Zhang, and Yueping Li. 2020. Session-Based Recommendation with Graph Neural Networks for Repeat Consumption. In *ICCP*. 519–524.
- [48] Zhen Yang, Ming Ding, Chang Zhou, Hongxia Yang, Jingren Zhou, and Jie Tang. 2020. Understanding Negative Sampling in Graph Representation Learning. In *SIGKDD*. 1666–1676.
- [49] David Yarowsky. 1995. Unsupervised Word Sense Disambiguation Rivaling Supervised Methods. In *ACL*. 189–196.
- [50] Yan Zhou, Murat Kantarcioglu, and Bhavani M. Thuraisingham. 2012. Self-Training with Selection-by-Rejection. In *ICDM*. 795–803.
- [51] Martin Zinkevich, Markus Weimer, Alexander J. Smola, and Lihong Li. 2010. Parallelized Stochastic Gradient Descent. In *NeurIPS*. 2595–2603.

A PROOF

A.1 Proof of Eq. (6)

PROOF. The first inequality of Eq. (6) is from the property of conditional expectation. Specifically, for a random variable $X = \nabla_{\theta} L(\tilde{Y}_i, \mathbf{F}_i) - \nabla_{\theta} L(Y_i, \mathbf{F}_i)$ and a partition of sampling space into two parts:

$$A = \{v_i \sim U(\mathcal{U}) | \tilde{Y}_i \neq Y_i\}$$

$$B = \{v_i \sim U(\mathcal{U}) | \tilde{Y}_i = Y_i\}$$

Then the following holds since $\mathbb{E}[X|B] = 0$:

$$\begin{aligned} \mathbb{E}[X] &= \mathbb{E}[X|A]P(A) + \mathbb{E}[X|B]P(B) \\ &= \mathbb{E}[X|A]P(A) \end{aligned}$$

Based on Jensen’s inequality, the first inequality of Eq. (6) holds.

$$\begin{aligned} \mathbb{E}[X] &= \|\mathbb{E}[X|A]P(A)\| \\ &\leq P(A)\mathbb{E}[\|X\| | A]. \end{aligned}$$

The second inequality is from the bounded gradient norm assumption and the triangle property of the norm, such that

$$\begin{aligned} \|\nabla_{\theta} L(\tilde{Y}_i, \mathbf{F}_i) - \nabla_{\theta} L(Y_i, \mathbf{F}_i)\| &\leq \|\nabla_{\theta} L(\tilde{Y}_i, \mathbf{F}_i)\| + \|\nabla_{\theta} L(Y_i, \mathbf{F}_i)\| \\ &\leq 2\Theta \end{aligned}$$

Then we have

$$\begin{aligned} \frac{|\mathcal{U}| \cdot P(A)}{|\mathcal{L}|} \cdot \mathbb{E}[\|X\| | B] &\leq \frac{2\Theta|\mathcal{U}|}{|\mathcal{L}|} \cdot P(A) \\ &= \frac{2\Theta|\mathcal{U}|}{|\mathcal{L}|} \cdot P_{v_i \sim U(\mathcal{U})}(\tilde{Y}_i \neq Y_i) \end{aligned}$$

Thus Eq. (6) holds. \square

B REPRODUCIBILITY

In what follows, we explain the details for reproducibility, including details of datasets, hardware and software versions used in our experiments, and hyper-parameter settings.

Our source code is at link: <https://anonymous.4open.science/r/e7aca211-0d8d-4564-8f3f-0ef24b01941e/>

We get the Cora, CiteSeer, PubMed, and Cora-full datasets from the following links provided by others. Our code will check these links and *automatically* download the data.

Cora, CiteSeer, and PubMed datasets at link:

<https://github.com/kimiyoung/planetoid/raw/master/data>

Cora-full dataset at link:

<https://github.com/abojchevski/graph2gauss/raw/master/data/>

B.1 Details of Datasets

Cora [39], Citeseer [39], Pubmed [39], and Core-full [1] are representative networks, widely used in existing studies [30, 31, 40] to benchmark the performance of semi-supervised learning tasks. For instance, in Cora, a node represents an article, and if two articles (nodes) have citation relationship, there is an edge between the two nodes in the corresponding graph. Every node has a bag-of-words (Cora, CiteSeer, Cora-full) or TF-IDF (PubMed) representation as the features of the node. Moreover, every node has a class label, representing the research area that the corresponding article belongs

Table 5: Hyper parameters and search space

Parameters	Search Space
Balancing	{True, False}
λ	{0.1, 1}
β	[0.1, 0.9] with step 0.1
λ_1	{0, 0.1, 0.3, 1, 3}
$(\mathcal{I} , \mathcal{J}_i)$	{(1, 10), (2, 5), (5, 2), (10, 1)}
L_2 regularization	{ $1e-2, 5e-3, 2e-3, 1e-3, 5e-4, 0$ }
Early Stopping	{True, False}
k in ABN_D	{10, 15, 20}
Dropout rate	{0.5, 0.8}

to. For instance, The class labels in Cora include Case Based Study, Genetic Algorithms, Neural Networks, Probabilistic Methods, Reinforcement Learning, Rule Learning, and Theory. The class labels in CiteSeer include Agents, AI, DB, IR, ML, HCI. The Cora-full dataset in [1] is an extended version of Cora with more nodes, edges, and classes.

B.2 Hardware and Software

In this section, we explain the hardware and software versions used in our experiments.

Hardware. We use a linux machine powered by a Intel(R) Xeon(R) E5-2603 v4 @ 1.70GHz CPU, associated with 131GB RAM, and installed with 4 Nvidia Geforce 1080Ti GPU Cards. Each 1080Ti card has 11GB GPU memory.

Software versions. The operating system is 16.04.1-Ubuntu SMP on x86_64. The Cuda version is 10.2.89. We use Python 3.7.4, and also use PyTorch 1.7.1 and Pytorch Geometric 1.6.0. In addition, we use the python packages including NetworkX, tqdm, DGL (cuda 10.2 version).

B.3 Hyper Parameters and Search Space

In this section, we explain the hyper parameters of ABN_G and ABN_D when instantiated over base models GCN and DAGNN respectively, and also introduce the search space of these parameters.

Table 5 summarizes the hyper parameters and their corresponding search space. We first tune the parameters of base models, and then tune the parameters of ABN. In particular, in terms of base models, we tune the following parameters: a L_2 regularization rate with search space in $\{1e-2, 5e-3, 1e-3, 5e-4, 1e-4, 5e-5, 0\}$, an early stopping enabler in {True, False}, a dropout rate in {0.5, 0.8}. In addition, for ABN_D , the level k of propagation after MLP is searched in {10, 15, 20}.

Further, we have the following parameter settings in our experiments: the number of hidden units of GCN and MLP (in DAGNN) is 64 units without bias; the number of layers of GCN and MLP (in DAGNN) is 2 layers; the learning rate of Adam Optimizer is 0.01; the activation function is RELU; the maximum number of training epochs is 1000. Moreover, early stopping is triggered when the validation loss is smaller than the average validation loss of previous 100 epochs, and the current epoch is beyond 500 epochs.

After finding the best hyper parameters of the base models on each classification task, we then tune the parameters of the three

techniques in ABN. In particular, adaptive pseudo labeling has a parameter β with search space in range [0.1, 0.9] with step 0.1, and a parameter λ controlling the weight of adaptive pseudo labels, with search space {0.1, 1}. Pseudo label balancing enabler searches values in {True, False}. Negative sampling regularization weight λ_1 is searched in {0, 0.1, 0.3, 1, 3}, and the number of positive and negative samples $(\mathcal{I}, \mathcal{J}_i)$ is searched in {(1, 10), (2, 5), (5, 2), (10, 1)}. For instance, (2, 5) means that we sample 2 positive nodes and then for each positive node, we sample 5 negative nodes.

B.4 Searched Hyper Parameters of ABN

In Tables 6 and 7, we present the searched hyper parameters of ABN_G and ABN_D on Cora and CiteSeer datasets respectively, in order to reproduce our results reported in Table 3 when varying the number of labels per class in {1, 3, 5, 10, 20}. Due to space limit, we only list the searched parameters on Cora and CiteSeer. Please find the searched parameters of ABN_G and ABN_D on all datasets including PubMed and Cora-full in our source code, to reproduce the results in experiments.

Table 6: The searched hyper parameters of ABN on Cora dataset

Parameters	ABN _G					ABN _D				
	1	3	5	10	20	1	3	5	10	20
# of labels per class	1	3	5	10	20	1	3	5	10	20
Balancing	True	True	True	False	False	True	True	True	False	False
λ	1	1	1	1	1	1	1	1	1	1
β	0.2	0.5	0.5	0.5	0.8	0.4	0.5	0.6	0.6	0.9
λ_1	1	0	1	1	0	1	1	1	0	1
$ \mathcal{I} $	5	0	5	2	0	5	2	10	0	10
$ \mathcal{J}_i $	2	0	2	5	0	2	5	1	0	1
L_2 regularization	0.0005	0.001	0.001	0.001	0.001	0.005	0.005	0.005	0.005	0.005
Early stopping	True	True	True	True	True	True	True	True	True	True
k in ABN _D	-	-	-	-	-	15	15	15	15	10
Dropout rate	0.8	0.8	0.8	0.8	0.8	0.8	0.8	0.8	0.8	0.8

Table 7: The searched hyper parameters of ABN on CiteSeer dataset

Parameters	ABN _G					ABN _D				
	1	3	5	10	20	1	3	5	10	20
# of labels per class	1	3	5	10	20	1	3	5	10	20
Balancing	True	True	True	True	True	True	True	True	True	True
λ	1	1	1	1	1	1	1	1	1	1
β	0.2	0.4	0.6	0.6	0.6	0.2	0.5	0.6	0.6	0.6
λ_1	0	3	3	1	1	1	1	0	0	0
$ \mathcal{I} $	0	5	5	2	2	5	2	0	0	0
$ \mathcal{J}_i $	0	2	2	5	5	2	5	0	0	0
L_2 regularization	0.0005	0.002	0.002	0.002	0.002	0.0005	0.005	0.005	0.02	0.02
Early stopping	True	True	True	True	True	True	True	True	True	True
k in ABN _D	-	-	-	-	-	15	15	15	15	10
Dropout rate	0.8	0.5	0.5	0.8	0.5	0.8	0.5	0.5	0.8	0.8